

Delving into the Adversarial Robustness on Face Recognition

Xiao Yang Dingcheng Yang Yinpeng Dong Wenjian Yu Hang Su Jun Zhu

Dept. of Comp. Sci. and Tech., Tsinghua University, Beijing, 100084, China
{yangxiao19,ydc19,dyp17}@mails.tsinghua.edu.cn, yu-wj@tsinghua.edu.cn,
{suhangss,dcszj}@mail.tsinghua.edu.cn

Abstract. Face recognition has recently made substantial progress and achieved high accuracy on standard benchmarks based on the development of deep convolutional neural networks (CNNs). However, the lack of robustness in deep CNNs to adversarial examples has raised security concerns to enormous face recognition applications. To facilitate a better understanding of the adversarial vulnerability of the existing face recognition models, in this paper we perform comprehensive robustness evaluations, which can be applied as reference for evaluating the robustness of subsequent works on face recognition. We investigate 15 popular face recognition models and evaluate their robustness by using various adversarial attacks as an important surrogate. These evaluations are conducted under diverse adversarial settings, including dodging and impersonation attacks, ℓ_2 and ℓ_∞ attacks, white-box and black-box attacks. We further propose a landmark-guided cutout (LGC) attack method to improve the transferability of adversarial examples for black-box attacks, by considering the special characteristics of face recognition. Based on our evaluations, we draw several important findings, which are crucial for understanding the adversarial robustness and providing insights for future research on face recognition. Code is available at <https://github.com/ShawnXYang/Face-Robustness-Benchmark>.

1 Introduction

Automatic face recognition is one of the most important research issues due to the rising concerns for public security, the need for identity verification, and the wide applications in multimedia data management. Recent progress in deep convolutional neural networks (CNNs) [34,37,17] has greatly facilitated the development of face recognition [39,36], with the state-of-the-art models by incorporating the margin-based loss functions [29,45,24,43,7] into deep CNN architectures. The excellent performance allows the face recognition models to be broadly applied in finance/payment, public access, criminal identification, *etc.*

However, recent research has found that the deep CNNs are highly vulnerable to adversarial examples [38,14], which are maliciously generated to make a model produce incorrect predictions. Unsurprisingly, the face recognition systems based on deep CNNs are also vulnerable to such adversarial examples. In

previous work, an adversarial eyeglass frame is generated to enable adversaries to evade being recognized or impersonate another identity when worn [32,33]. A recent work breaks into a commercial face recognition API by generating adversarial examples in a black-box manner [13]. As a result, the vulnerability of the face recognition systems against adversarial examples offers many challenges and security issues in real-world task-critical applications. For example, a payment face recognition system fooled by adversarial examples could lead to severe consequences. Therefore, it is of significant importance to benchmark the adversarial robustness of the existing face recognition models under various settings, which will provide a better understanding of their robustness and provide insights for the design of more robust models in facial tasks, as well as in other metric learning tasks such as image retrieval [6], person re-identification [44], *etc.*

A common approach to evaluate the adversarial robustness of models is adopting adversarial attacks as a surrogate, since they can identify the vulnerability of the models by generating the worst-case adversarial examples [3,26]. A lot of methods [38,14,23,11] have been proposed to perform adversarial attacks and evaluate the robustness on the general image classification tasks. However, on face recognition, although various studies have demonstrated the vulnerability of the face models against adversarial attacks, they only concentrate on a limited number of scenarios, such as physical realizable attacks [32] and decision-based black-box attacks [13]. There still lacks a comprehensive and rigorous evaluation of the adversarial robustness of the existing face models, thus little is known whether there exists a *trade-off* between the robustness and accuracy of the current popular face models. Therefore, we need to define appropriate attack objectives and evaluation criteria to fully measure the robustness of face recognition in diverse adversarial settings.

In this paper, we establish a comprehensive and rigorous evaluation method of the adversarial robustness on face recognition. We build white-box and black-box attack settings on public datasets and evaluate the adversarial robustness of various representative face models, to examine which factors (e.g., model architecture, training objective) could influence their adversarial robustness. That provides an overall understanding of the robustness of the existing face recognition models and facilitate the future research. Specifically, we study the robustness on *face verification* under the ℓ_p additive noises [14], since this setting is well-defined and widely recognized [2]. We incorporate 15 popular face recognition models for robustness evaluations, which cover most of models trained by representative losses and network architectures. To evaluate their robustness, we adopt distortion, robustness curves, and transferability of the adversarial examples as evaluation metrics under a complete set of settings, including dodging and impersonation attacks, ℓ_2 and ℓ_∞ attacks, as well as white-box and black-box attacks, which are recommended as the evaluate criteria for robustness of the future works on face recognition.

Moreover, in order to improve the performance of black-box attacks to better understand the robustness of the face models in the black-box manner, we further propose a *landmark-guided cutout* (LGC) attack method by considering

the special characteristics of face recognition. Our method makes the generated adversarial examples less sensitive to the local discriminative region, thus fooling other black-box face recognition models more effectively. The proposed LGC can be also integrated into any black-box attack method to improve the baseline.

By analyzing the evaluation results, we have some meaningful findings. First, currently most popular models with glorious precision, e.g. ArcFace and CosFace, do not have a crucial and consistent effect than other losses on robustness, which is inconsistent with the conclusion of evaluating the robustness on the Imagenet classification task that robustness is scarified when pursuing a higher classification performance [35]. Second, model architecture is a more critical factor for robustness than other factors, e.g., loss functions. Selecting a proper larger network structure as a backbone usually exhibit better resistance against adversarial examples, which also provides an insight for robustness. Third, the models with similar architectures (in the same model family) have good adversarial transferability against each other. We also find that the adversarial examples generated against IResNet [8] are more transferable to other face models. Fourth, the proposed landmark-guided cutout (LGC) makes the generated adversarial examples less sensitive to the discriminative region based on the characteristics of face recognition. After integrated into momentum iterative method (MIM) [11], LGC attack has the best black-box attack performance currently. More analyses of the results are provided in Sec. 4.3.

2 Background and Evaluation Settings

In this section, we introduce the background knowledge and robustness evaluation criteria on face recognition.

2.1 Threat Models

Let $f(\mathbf{x}) : \mathcal{X} \rightarrow \mathbb{R}^d$ denote a face recognition model that extracts a normalized feature representation in \mathbb{R}^d for an input face image $\mathbf{x} \in \mathcal{X} \subset \mathbb{R}^n$. Face verification aims to compute the distance between the feature representations of a pair of face images. Given $\{\mathbf{x}_1, \mathbf{x}_2\} \subset \mathcal{X}$, we first denote their feature distance as $\mathcal{D}_f(\mathbf{x}_1, \mathbf{x}_2)$, where \mathcal{D}_f is usually defined as

$$\mathcal{D}_f(\mathbf{x}_1, \mathbf{x}_2) = \|f(\mathbf{x}_1) - f(\mathbf{x}_2)\|_2^2. \quad (1)$$

So the verification result $\mathcal{C}(\mathbf{x}_1, \mathbf{x}_2)$ given the pair of face images $\{\mathbf{x}_1, \mathbf{x}_2\}$ can be formally expressed as

$$\mathcal{C}(\mathbf{x}_1, \mathbf{x}_2) = \mathbb{I}(\mathcal{D}_f(\mathbf{x}_1, \mathbf{x}_2) < \delta), \quad (2)$$

where \mathbb{I} is the indicator function, and δ is a threshold. When $\mathcal{C}(\mathbf{x}_1, \mathbf{x}_2)$ equals to 1, the pair of images are predicted to be the same identity. Otherwise, they are regarded as different identities. Note that this definition is consistent with the commonly used cosine similarity metric for face verification, since f outputs a normalized feature for an input.

Given the face verification model, the adversary can have different goals, capabilities, and knowledge [2] for generating adversarial examples. Below we introduce these three aspects, respectively.

Adversary’s goals. We focus on two types of attacks with different goals. On one hand, *dodging attacks* correspond to generating an adversarial example that is recognized wrong or not recognized. For face verification, given a pair of face images $\{\mathbf{x}, \mathbf{x}^r\}$ with the *same* identity, the adversary seeks to modify \mathbf{x} to generate an adversarial image \mathbf{x}^{adv} and make the model recognize \mathbf{x}^{adv} and \mathbf{x}^r as not the same identity. So the goal is making $\mathcal{C}(\mathbf{x}^{adv}, \mathbf{x}^r) = 0$. On the other hand, *impersonation attacks* aim to generate an adversarial example that is recognized as a specific identity, which could be used to evade the face authentication systems. For face verification, given a pair of face images $\{\mathbf{x}, \mathbf{x}^r\}$ with the *different* identities, the adversary tries to find an adversarial image \mathbf{x}^{adv} that is recognized as the same identity of \mathbf{x}^r . So the goal is to make $\mathcal{C}(\mathbf{x}^{adv}, \mathbf{x}^r) = 1$.

Adversary’s capabilities. As adversarial examples are usually assumed to be indistinguishable from the corresponding original ones to human eyes [38,14], the adversary can only make small changes to the inputs. In this paper, we study the well-defined and widely used ℓ_p additive perturbation setting, where the adversary is allowed to add a small perturbation measured by the ℓ_p norm to the original input. Specifically, we consider the ℓ_∞ and ℓ_2 norms.

To achieve the adversary’s goal, we optimize the feature distance between the adversarial image \mathbf{x}^{adv} and the other face image \mathbf{x}^r , and keep a small distance between \mathbf{x}^{adv} and \mathbf{x} in the input space. For dodging attacks, an adversarial image can be generated by solving the constrained optimization problem as

$$\mathbf{x}^{adv} = \arg \max_{\mathbf{x}': \|\mathbf{x}' - \mathbf{x}\|_p \leq \epsilon} \mathcal{D}_f(\mathbf{x}', \mathbf{x}^r), \quad (3)$$

where ϵ is a small constant. By solving Eq. (3), the feature distance between \mathbf{x}^{adv} and \mathbf{x}^r is maximized, such that the face verification model would misclassify them as being different identities when their feature distance exceeds the threshold δ . For impersonation attacks, we can similarly solve

$$\mathbf{x}^{adv} = \arg \min_{\mathbf{x}': \|\mathbf{x}' - \mathbf{x}\|_p \leq \epsilon} \mathcal{D}_f(\mathbf{x}', \mathbf{x}^r). \quad (4)$$

Therefore, the feature representation of \mathbf{x}^{adv} will resemble that of \mathbf{x}^r , such that the face verification model would classify them as the same identity.

Adversary’s knowledge. An adversary can have different levels of knowledge of the target model to craft adversarial examples. Besides the white-box access to the model architectures and parameters, the black-box attack scenario is another important setting to evaluate the robustness, since the black-box attack setting is more practical in real-world applications. So we consider both *white-box attacks* and *black-box attacks* in this paper.

White-box attacks rely on detailed information of the target model, including architecture, parameters, and gradient of the loss with respect to the input.

Black-box attacks can be realized based on the transferability of adversarial examples [27]. Transfer-based black-box attacks do not rely on model information but assume the availability of a substitute model, from which the adversarial examples are generated. Note that there also exist query-based black-box attacks [4,13], which leverage the query feedback of the target model to generate adversarial examples. However, we do not consider query-based black-box attacks in this paper and leave this study to future work.

2.2 Face Recognition Models

Due to the development of deep CNNs, face recognition has obtained remarkable progress recently. DeepFace [39] and DeepID [36] regard face recognition as a multi-class classification problem and train deep CNNs supervised by the softmax loss to learn features. The state-of-the-art methods treat face recognition as a metric learning problem and learn highly discriminative features by margin-based loss functions. The triplet loss [29] and the center loss [45] are proposed to increase the Euclidean margin in the feature space between classes. Moreover, SphereFace [24] uses the angular softmax loss, CosFace [43] uses the large margin cosine loss, and ArcFace [7] uses the additive angular margin loss, to improve the margin in the angular space for achieving good performance.

To effectively evaluate the robustness of face recognition models, we choose 15 representative and state-of-the-art face recognition models, covering different model architectures, training objective functions, and the best publicly available models. To measure the effects of model architectures, we train many models under different backbones with different size of weights, including MobileFace [5], MobileNet [19], MobileNetV2 [28], ShuffleNetV1 [49], ShuffleNetV2 [25], and ResNet50 [18], which are trained by the softmax loss. To measure the effects of training objectives, we include the models of the same IResNet50 [8] architecture optimized by distance-based losses, such as softmax and FaceNet [29], and those optimized by angle-based losses, such as Sphreface [24], AM-softmax [42], CosFace [43], and ArcFace [8]. Besides, we also include the publicly available models FaceNet, SphereFace, CosFace, and ArcFace for more comprehensive evaluations.

For each dataset used in our evaluations, we compute the threshold¹ in Eq. (2) of each model that gives the highest accuracy on the test set. The detailed information of these models are shown in Table 1.

2.3 Datasets

We perform adversarial robustness evaluations on the Labeled Face in the Wild (LFW) [20] and YouTube Faces Database (YTF) [46] in this paper, which are two of the most widely used benchmark datasets for face verification on images and videos. Besides, we also report the evaluation results on a more challenging dataset named the Celebrities in Frontal-Profile (CFP) dataset [31].

¹ The relationship of the Euclidean threshold δ_d and the Cosine threshold δ_c after normalizing features is $\delta_d = 2 - 2 \cdot \delta_c$, where $\delta_d \in [0, 4]$.

Models	Method	Backbone	Loss	Accuary	Threshold
FaceNet	Public	InceptionResNetV1	Triplet	0.992	1.159
SphereFace	Public	Sphere20	A-Softmax	0.982	1.301
CosFace	Public	Sphere20	LMCL	0.987	1.507
ArcFace	Public	IR-SE50	Arcface	0.995	1.432
MobleFace	Trained	MobileFaceNet	Softmax	0.995	1.578
MobileNet	Trained	MobileNet	Softmax	0.994	1.683
MobileNetv2	Trained	MobileNetv2	Softmax	0.993	1.547
ShuffleNetV1	Trained	ShuffleNetV1	Softmax	0.995	1.619
ShuffleNetV2	Trained	ShuffleNetV2	Softmax	0.992	1.552
ResNet50	Trained	ResNet50	Softmax	0.997	1.618
Softmax-IR	Trained	IResNet50	Softmax	0.996	1.315
SphereFace-IR	Trained	IResNet50	A-softmax	0.996	1.277
AM-IR	Trained	IResNet50	AM-softmax	0.992	1.083
CosFace-IR	Trained	IResNet50	LMCL	0.997	1.552
ArcFace-IR	Trained	IResNet50	ArcFace	0.997	1.445

Table 1. The face recognition models adopted for robustness evaluation in this paper. We show their accuracy on the LFW dataset [20] using the best threshold.

LFW. LFW dataset is the most widely used benchmark for face verification on images, which contains 13,233 face images from 5,749 different individuals. LFW includes faces with various pose, expression, and illuminations. The *unrestricted with labeled outside data* protocol includes 6,000 face pairs, including 3,000 pairs with the same identities and 3,000 pairs with different identities.

YTF. YTF dataset includes 3,424 videos from 1,595 different people. All of the video sequences are from Youtube, and the average length of a video clip of YTF is about 181 frames. The unrestricted with labeled outside data protocol contains 5,000 video pairs, half of which belong to the same identities and the others come from different identities.

CFP-FP. CFP-FP dataset isolates pose variation with extreme poses like profile, where many features are occluded. The dataset contains 10 frontal and 4 profile images of 500 individuals. Similar to LFW, the standard data protocol has defined 10 splits, and contains 350 pairs with the same identities and 350 pairs with different identities.

Implementation details. We perform dodging attacks based on the pairs of images with the same identities, and impersonation attacks based on the pairs with different identities. We first use MTCNN [48] to detect face area and align images for the entire images. Then, we obtain the cropped faces which are resized to 112×112 . Note that the specific input size and pixel transformation will be executed inside each model due to the diversity of model inputs. All trained models are based on the MS-Celeb-1M dataset [15].

2.4 Evaluation Criteria

Given an attack method $\mathcal{A}_{\epsilon,p}$ that generates an adversarial example $\mathbf{x}^{adv} = \mathcal{A}_{\epsilon,p}(\mathbf{x}, \mathbf{x}^r)$ for an input \mathbf{x} and a reference image \mathbf{x}^r with perturbation budget ϵ

under the ℓ_p norm ($\|\mathbf{x}^{adv} - \mathbf{x}\|_p \leq \epsilon$), the first evaluation criterion is the attack success rate of the attack on the face recognition model \mathcal{C} in Eq. (2), defined as

$$\text{Asr}(\mathcal{C}, \mathcal{A}_{\epsilon,p}) = \frac{1}{N} \sum_{i=1}^N \mathbb{I}(\mathcal{C}(\mathcal{A}_{\epsilon,p}(\mathbf{x}_i, \mathbf{x}_i^r), \mathbf{x}_i^r) \neq y_i), \quad (5)$$

where $\{\mathbf{x}_i, \mathbf{x}_i^r\}_{i=1}^N$ is the paired test set, y_i takes 1 if $\{\mathbf{x}_i, \mathbf{x}_i^r\}$ belongs to same identity, and 0 otherwise.

The second evaluation criterion is the (median) *minimum distance of the adversarial perturbations*, which is a simple metric to show the worst-case robustness of the models [1]. To obtain this value for each data, we perform a binary search on ϵ to find its minimum value that fulfills the adversary’s goal. The third evaluation criterion is the *attack success rate vs. perturbation budget curve*, which can give a global understanding of the robustness of face recognition models [10]. To obtain this curve, we need to calculate attack success rate for all values of ϵ , which can be efficiently done by finding the minimum perturbations and counting the number of the adversarial examples, the ℓ_p norm of whose perturbations is smaller than each ϵ . We use different criteria for different attacks, which will be specified in Sec. 4.

3 Attack Methods

In this section, we introduce several adversarial attack methods that are adopted for robustness evaluation. We further propose a novel landmark-guided cutout (LGC) method to improve the transferability of adversarial examples by considering the special characteristics of face recognition.

3.1 Typical Attack Methods

To solve Eq. (3) or Eq. (4), many methods can be used to generate adversarial examples. In this section, we summarize the typical adversarial attack methods. We only introduce these methods for dodging attacks, since the extension to impersonation attacks is straightforward, given the similar problem formulations in Eq. (3) and Eq. (4).

Fast Gradient Sign Method (FGSM) [14] generates an adversarial example given a pair of images $\{\mathbf{x}, \mathbf{x}^r\}$ with the same identity under the ℓ_∞ norm as

$$\mathbf{x}^{adv} = \mathbf{x} + \epsilon \cdot \text{sign}(\nabla_{\mathbf{x}} \mathcal{D}_f(\mathbf{x}, \mathbf{x}^r)), \quad (6)$$

where $\nabla_{\mathbf{x}} \mathcal{D}_f$ is the gradient of the feature distance with respect to \mathbf{x} . $\text{sign}(\cdot)$ is the sign function to make the perturbation meet the ℓ_∞ norm bound. It can be extended to an ℓ_2 attack as

$$\mathbf{x}^{adv} = \mathbf{x} + \epsilon \cdot \frac{\nabla_{\mathbf{x}} \mathcal{D}_f(\mathbf{x}, \mathbf{x}^r)}{\|\nabla_{\mathbf{x}} \mathcal{D}_f(\mathbf{x}, \mathbf{x}^r)\|_2}. \quad (7)$$

Basic Iterative Method (BIM) [22] extends FGSM by iteratively taking multiple small gradient updates as

$$\mathbf{x}_{t+1}^{adv} = \text{clip}_{\mathbf{x}, \epsilon}(\mathbf{x}_t^{adv} + \alpha \cdot \text{sign}(\nabla_{\mathbf{x}} \mathcal{D}_f(\mathbf{x}_t^{adv}, \mathbf{x}^r))), \quad (8)$$

where $\text{clip}_{\mathbf{x}, \epsilon}$ projects the adversarial example to satisfy the ℓ_∞ constrain and α is the step size. It can also be extended to an ℓ_2 attack similar to FGSM. The projected gradient descent (PGD) [26] is also a variant of BIM by using random starts, and we only adopt BIM for evaluations since PGD and BIM result in similar attack performance. It has been shown that BIM is not good at generating transferable adversarial example [11].

Momentum Iterative Method (MIM) [11] integrates a momentum term into BIM for improving the transferability of adversarial examples as

$$\begin{aligned} \mathbf{g}_{t+1} &= \mu \cdot \mathbf{g}_t + \frac{\nabla_{\mathbf{x}} \mathcal{D}_f(\mathbf{x}_t^{adv}, \mathbf{x}^r)}{\|\nabla_{\mathbf{x}} \mathcal{D}_f(\mathbf{x}_t^{adv}, \mathbf{x}^r)\|_1}; \\ \mathbf{x}_{t+1}^{adv} &= \text{clip}_{\mathbf{x}, \epsilon}(\mathbf{x}_t^{adv} + \alpha \cdot \text{sign}(\mathbf{g}_{t+1})). \end{aligned} \quad (9)$$

MIM can be similarly extended to the ℓ_2 case.

Carlini & Wagner’s Method (C&W) [3] is a powerful optimization-based attack method. It takes a Lagrangian form of the constrained optimization problem and adopts Adam [21] for optimization. This method is very effective for ℓ_2 attacks. However, the direct extension of the C&W method to face verification is problematic since C&W uses the loss function defined on the logits of the classification models. In face verification, there is no logit output of the face models. Therefore, we define a new attack objective function suitable for face verification systems. For dodging attacks, the optimization problem can be formulated as

$$\mathbf{x}^{adv} = \arg \min_{\mathbf{x}'} \{ \|\mathbf{x}' - \mathbf{x}\|_2^2 + c \cdot \max(\delta - \mathcal{D}_f(\mathbf{x}', \mathbf{x}^r), 0) \}, \quad (10)$$

where c is a parameter to balance the two loss terms, whose optimal value is found by binary search. Recall that δ is the threshold of the face verification model in Eq. (2). C&W is not good at ℓ_∞ attacks [3], so we only use it under the ℓ_2 norm.

Transfer-based Black-box Attacks. Under this setting, we generate adversarial examples by using the above methods against a substitute face models, and use them to attack the black-box models. For the studied 15 face models in our evaluations, we treat each one as the white-box model to generate adversarial examples and test the performance against the other models.

3.2 Landmark-Guided Cutout

Although the above attack methods can be used for attacking face models, they are originally designed on the general image classification tasks. The adversarial examples can be highly associated with the local discriminative region of the white-box model for an input image, as emphasized in [12]. The normally trained

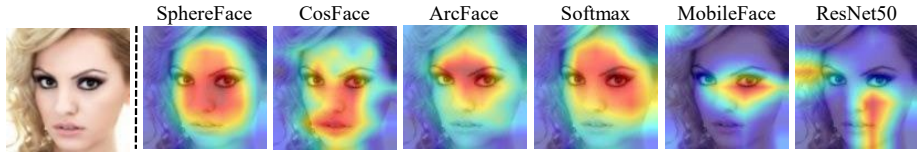


Fig. 1. The illustration of the attention maps of the different models. We employ Grad-Gram [30] which produces the attention maps highlighting the discriminative regions.

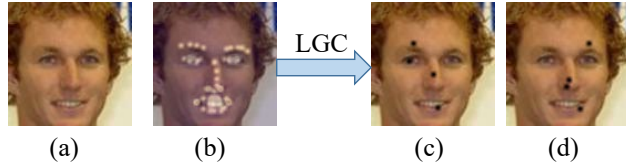


Fig. 2. The illustration of the landmark-guided cutout method, where (a) is the original input, (b) has fixed number of landmarks. We randomly sample face landmarks in (b) as a mask in the process of generating adversarial examples, e.g., (c) and (d).

image classification models generally have similar discriminative regions, making the crafted adversarial examples have a high transferability [41,12]. However, we find that the existing SOTA face recognition models have different attention maps for their predictions given the same input image, as illustrated in Fig. 1. Therefore, the crafted adversarial examples will depend on the local discriminative region of the white-box model, making it difficult to transfer to the black-box models with different discriminative regions.

To weaken the effect of different discriminative regions for the overall transferability, we further propose a **landmark-guided cutout** (LGC) attack method. The *cutout* method [9] has been proven that it can make models take image context into consideration by randomly occluding units at the input space. Therefore, selecting appropriate occlusion from key positions can reduce sensibility of discriminative regions in the process of generating adversarial examples. Many researches have also shown that there exist some important regions for face recognition, including the surroundings of eyes and noses [40,16,47], which are also consistent with the overall prominent regions shown in Fig. 1. Thus we extend *cutout* to the proposed LGC method, which occludes units from *prominent* regions from the input of the images, making the network focus on less prominent regions and obtain more transferable adversarial examples. To achieve this goal, we apply a spatial prior by locating face landmarks by using face landmark detection [16], as illustrated in Fig. 2. Specifically, we apply a fixed-size mask to randomly sampled M locations as center points from face landmarks, and place a square patch around those locations. A simple combination of BIM and landmark-guided cutout can give rise to the landmark-guided cutout iterative method as

$$\mathbf{x}_{t+1}^{adv} = \text{clip}_{\mathbf{x},\epsilon}(\mathbf{x}_t^{adv} + \alpha \cdot \text{sign}(\nabla_{\mathbf{x}} \mathcal{D}_f(M_t \odot \mathbf{x}_t^{adv}, \mathbf{x}^r))), \quad (11)$$

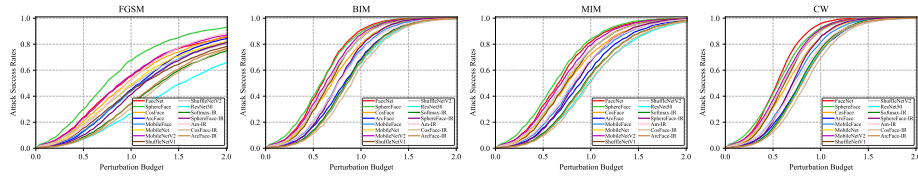


Fig. 3. The *attack success rate vs. perturbation budget* curves of the 15 models against dodging attacks under the ℓ_2 norm.

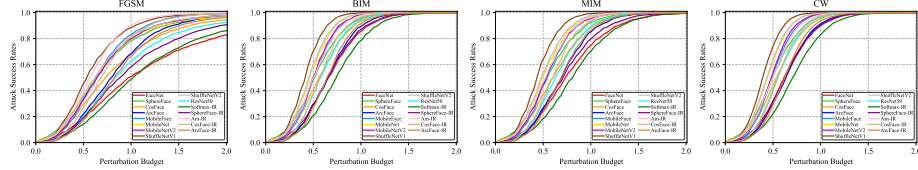


Fig. 4. The *attack success rate vs. perturbation budget* curves of the 15 models against impersonation attacks under the ℓ_2 norm.

where $M_t \in \{0, 1\}^d$ is a binary mask and \odot is the element-wise dot product. In the t -th iteration, some randomly sampled fixed-size small square regions are set to 0 to form M_t .

	ℓ_2								ℓ_∞					
	FGSM		BIM		MIM		C&W		FGSM		BIM		MIM	
	dod. imp.	dod. imp.	dod. imp.	dod. imp.	dod. imp.									
FaceNet	0.92	1.17	0.59	0.66	0.66	0.73	0.54	0.61	1.75	2.14	1.17	1.31	1.28	1.42
SphereFace	0.73	0.64	0.58	0.52	0.62	0.55	0.56	0.50	1.31	1.11	1.06	0.92	1.12	0.97
CosFace	0.97	0.73	0.69	0.56	0.75	0.59	0.65	0.54	1.69	1.25	1.30	1.00	1.39	1.06
ArcFace	1.09	0.80	0.83	0.66	0.89	0.69	0.79	0.64	1.97	1.42	1.53	1.20	1.62	1.25
MobileFace	1.11	0.62	0.75	0.50	0.83	0.53	0.71	0.49	1.98	1.12	1.44	0.94	1.55	0.97
MobileNet	1.03	0.64	0.67	0.47	0.73	0.50	0.62	0.44	1.75	1.08	1.22	0.83	1.31	0.88
MobileNetV2	0.89	0.64	0.62	0.50	0.69	0.53	0.59	0.48	1.55	1.12	1.17	0.91	1.25	0.95
ShuffleNetV1	1.12	0.53	0.67	0.41	0.75	0.44	0.62	0.39	2.02	0.97	1.28	0.77	1.39	0.80
ShuffleNetV2	1.06	0.62	0.66	0.45	0.72	0.48	0.61	0.43	1.86	1.08	1.23	0.84	1.31	0.88
ResNet50	1.53	0.84	0.86	0.58	0.97	0.62	0.79	0.55	2.64	1.44	1.59	1.05	1.75	1.11
Softmax-IR	1.30	1.05	0.84	0.73	0.94	0.81	0.78	0.71	2.36	1.86	1.66	1.41	1.80	1.50
SphereFace-IR	1.14	0.90	0.77	0.66	0.84	0.70	0.70	0.63	2.12	1.62	1.50	1.25	1.62	1.31
Am-IR	0.95	0.56	0.77	0.50	0.81	0.52	0.74	0.49	1.67	1.00	1.41	0.92	1.47	0.94
CosFace-IR	1.33	0.69	0.91	0.56	0.98	0.59	0.85	0.55	2.45	1.27	1.78	1.09	1.91	1.14
ArcFace-IR	1.28	0.83	0.86	0.64	0.95	0.69	0.81	0.62	2.39	1.55	1.72	1.25	1.84	1.31

Table 2. The median distance of the *minimum perturbations* of the 15 models against dodging and impersonation attacks under the ℓ_2 and ℓ_∞ norms.

4 Evaluation Results

We present the evaluation results on LFW in this section. Due to the the space limitation, we leave the results on YTF and CFP-FP datasets in Appendix C. Since the input size is different for each face model, we adopt the normalized ℓ_2 distance defined as $\bar{\ell}_2(\mathbf{a}) = \frac{\|\mathbf{a}\|_2}{\sqrt{d}}$ as the measurement for ℓ_2 attacks, where d is the dimension of a vector \mathbf{a} . We set $\alpha = 1.5\epsilon/T$ for iterative attack methods,

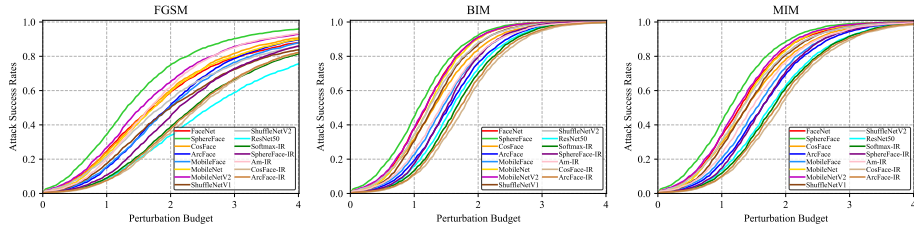


Fig. 5. The *attack success rate vs. perturbation budget* curves of the 15 models against dodging attacks under the ℓ_∞ norm.

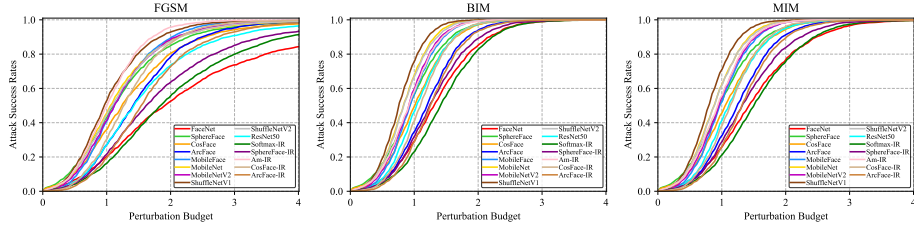


Fig. 6. The *attack success rate vs. perturbation budget* curves of the 15 models against impersonation attacks under the ℓ_∞ norm.

where T is the maximum iteration. And we set $\mu = 1.0$ for MIM and $c = 10^{-3}$ for C&W. For LGC, the mask consists of four squares with a radius of 3, and each square uses a randomly selected key point as the center. We compare LGC with a baseline called *cutout iterative method* (CIM) that performs random cutout in Appendix A. We also discuss the effect of different numbers and size lengths of the mask squares of LGC in Appendix B. For black-box attacks, we test the transferability of adversarial examples between each pair of the face models.

4.1 White-box Evaluation Results

We fixed the attack iterations as 20 for BIM and MIM and 100 for C&W. To get minimum perturbation, a binary search with 10 iterations is used after finding a feasible adversarial example by linear search. We show the *attack success rate vs. perturbation budget* curves of the 15 models against FGSM, BIM, MIM, and C&W attacks under the ℓ_2 norm in Fig. 3 and Fig. 4, and the curves of FGSM, BIM, MIM under the ℓ_∞ norm in Fig. 5 and Fig. 6. Table 2 shows the median distance of the minimum perturbations under the same settings.

Relationship between precision and robustness. For dodging and impersonation attacks, the success rate of FGSM is very pool while C&W attack gets the best performance, which accords with the performance on the general image classification [10,35]. However, we observe that those methods with the glorious precision, e.g., ArcFace and CosFace, do not have a crucial and consistent effect on robustness, which is inconsistent with the conclusion of evaluating robustness for the Imagenet classification task where there exists a trade-off between precision and robustness. Specifically, ArcFace and CosFace with the I-ResNet architecture perform differently on dodging and impersonation settings.

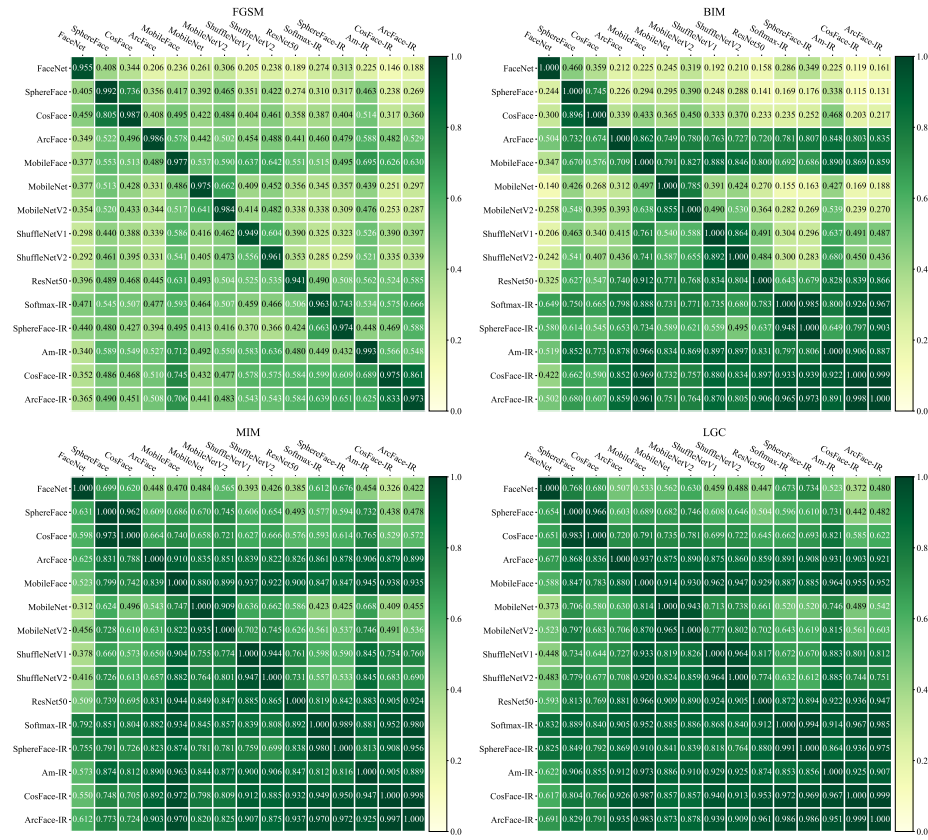


Fig. 7. The attack success rates of the 15 models against black-box dodging attacks under the ℓ_∞ norm.

They exhibit better defensive performance against dodging attacks compared with other losses such as softmax, yet not very well against impersonation attacks. Therefore, this is worth noting that learning more discriminative features from the metric space for precision cannot substantially improve robustness.

Effects of different factors. On the whole, model architecture is a more critical factor for robustness than loss functions. The models with a larger size of weights are more resistant to dodging and impersonation attacks under both norms. For instance, the models with the IResNet architecture have better robustness than light-weight models under all white-box settings. Therefore, selecting a proper larger network structure as a backbone usually leads to better resistance against adversarial examples, which also provides an insight for robustness.

4.2 Black-box Evaluation Results

For black-box attacks, we fix the perturbation budget as $\epsilon = 8$ for ℓ_∞ attacks and $\epsilon = 4$ for ℓ_2 attacks. Considering that black-box attacks are harder than white-box attacks, we perform 100 iterations for iterative attacks. We show the *attack success rate* of the 15 models against dodging and impersonation attacks based on black-box FGSM, BIM, MIM, and LGC methods under the ℓ_∞ norm in Fig. 7 and Fig. 8. In this experiment, we choose a model as the substitute model to attack the others. The value in the i -th row and the j -th column of each heatmap matrix is the attack success rate for the target model j on the adversarial examples generated by the source model i .

Performance analysis. We observe that the same model has a similar overall transferable trend for different attack methods. Obviously, LGC improves the transferability of adversarial examples over FGSM, BIM, and MIM, resulting in a higher attack success rate against the black-box models. Therefore, landmark-guided prior knowledge is beneficial for exploring transferable adversarial examples for the face recognition task.

Robustness of different models. We observe that model architecture is a very important factor for robustness. Those models within the same architecture family have good transferability across each other. The models with light weights (e.g., MobileNet and ShuffleNet) are easily attacked by the adversarial examples generated against other models. The models within IResNet50 family have the strongest transferability. One potential reason is that many networks (e.g., MobileNet and ShuffleNet) are based on improvements in the residual unit.

Robustness of different optimization loss. We study the effect of different loss functions based on the IResNet structure. We observe that models among Am-IR, CosFace-IR and ArcFace have mutual transferability because their metric optimizations lie in angular space combined with additive margin. Therefore, we claim that adversarial samples obtained by similar training methods have stronger mobility.

In our setting, FaceNet is the most difficult one to transfer to other models, which is trained on InceptionResNetV1 network based on the triplet loss in the Euclidean space. The model architecture and training objection of FaceNet are very different from those models with basic residual structure and angular space. This might provide new valuable insights for designing robust models against black-box attacks that selecting diverse backbones and train function will restrict the transferability of adversarial samples by common white-box recognition models.

4.3 Discussions

Based on the evaluation results, we highlight some key findings.

First, current mainstream direction on face recognition that learning more discriminative features from the metric space, e.g., ArcFace and CosFace, cannot substantially improve robustness. Targeted exploration of designing models is significantly taking into account robustness.

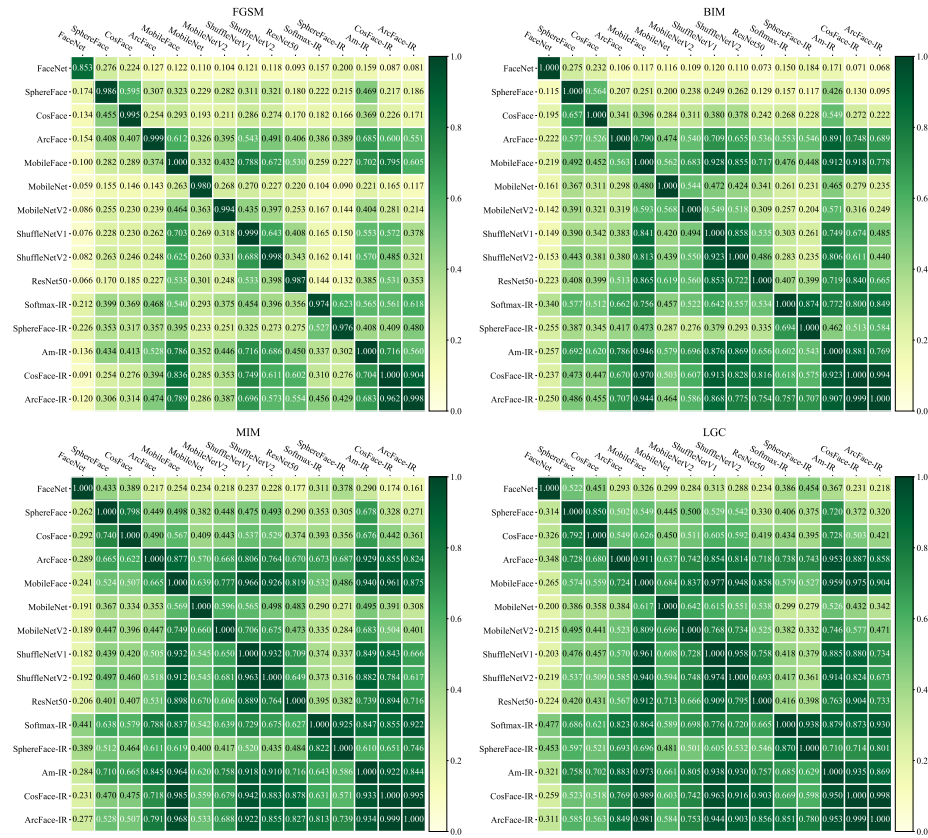


Fig. 8. The attack success rates of the 15 models against black-box impersonation attacks under the ℓ_∞ norm.

Second, we observe model architecture is a more critical factor, light-weight models, e.g., MobileNet and ShuffleNet, have worse defensive performance than those of normal weights under all white-box and black-box settings. Therefore, selecting a suitable larger network structure as a backbone seems more effective for robustness.

Third, we observe that the models with similar structures have a higher attack success rate for transferability. Besides, similar training methods are also mutually transferable, such as CosFace, ArgFace, and Am-softmax.

Fourth, the attack performance under ℓ_2 and ℓ_∞ norms is similar in generalization ability. The difficulty of impersonation attacks is higher than that of dodging attacks.

Fifth, our proposed landmark-guided cutout (LGC) makes the generated adversarial examples more transferable based on the characteristics of face tasks, which can be applied to any black-box attack method. After combining with MIM, LGC is also the best baseline currently.

5 Conclusion

To the best of our knowledge, we performed the largest experiment on evaluating the adversarial robustness on *face recognition*. We tested the performance of various face recognition models with different model architectures or training objectives against both white-box and black-box attacks. We also proposed a novel landmark-guided cutout method to further improve the transferability of the generated adversarial examples. We conjecture that robustness should also be considered in model designs while pursuing higher accuracy, and we also provide thorough evaluation criteria on face recognition for the robustness of the future works. We believe that our findings could provide insights to the adversarial robustness issue of face recognition, and even in other metric learning tasks such as image retrieval, person re-identification, and so on.

A Comparison of CIM and LGC.

We compare the performance of Cutout (CIM) and Landmark-Guided Cutout (LGC) on the LFW dataset. For CIM, we apply a square zero-mask with a side length of 10 [9] to a random location at each iteration. As for LGC, the mask consists of four small squares, making a randomly selected key face landmark as the center. Note that we ensure that the total mask area used for CIM and LGC is equal. Fig. 9 and Fig. 10 show the success rates of the 15 models against black-box dodging and impersonation attacks based on CIM and LGC under the ℓ_∞ norm. LGC achieves more performance under the dodging and impersonation setting. The results also demonstrate that the adversarial examples generated by LGC are less sensitive to the discriminative regions, thus fooling other black-box face recognition models.

B Different Quantities and Sizes for LGC

In this section, we discuss the impact of different quantities and sizes on LGC. We choose a model from 15 models as the substitute model to attack the others. Fig. 11 and Fig. 12 show the success rates of different models against black-box dodging and impersonation attacks under different *quantities* of black-squares for LGC. Fig. 13 and Fig. 14 show the success rates of different models against black-box dodging and impersonation attacks under different *sizes* of black-squares for LGC. The value in the i -th row and the j -th column of each heatmap matrix implies the attack success rate for the target model j on the adversarial samples generated by the source models i . We found that the best results can be achieved only with the appropriate quantities and sizes of occlusions. Too big or too small is not optimal.

C Full Evaluation Results

In addition to the LFW dataset mentioned, we also perform an adversarial evaluation on YouTube Faces Database (YTF) [46]. Besides, experiments on larger

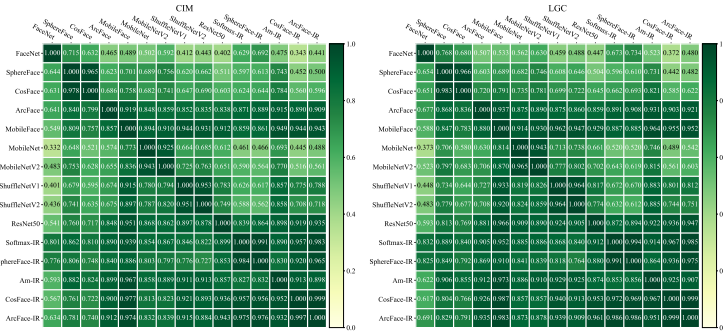


Fig. 9. The success rates of the 15 models against black-box dodging attacks based on CIM and LGC under the ℓ_∞ norm.

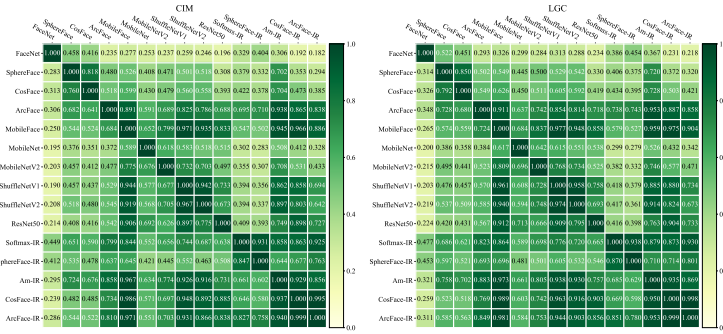


Fig. 10. The success rates of the 15 models against black-box impersonation attacks based on CIM and LGC under the ℓ_∞ norm.

and more challenging face verification datasets, e.g., CFP-FP [31], are shown in the following section.

C.1 Evaluation on the YTF dataset

YTF contains 5000 video pairs, half of which belong to the same identities and others come from different identities. We select an intermediate frame as the representative image to perform our task. We perform dodging attacks based on the pairs of images with the same identities, and impersonation attacks based on the pairs with different identities. The parameter setting is the same as LFW.

White-box attacks: We show some robustness curves for white-box attacks and provide attack success rate vs. perturbation budget of face recognition models against dodging and impersonation attacks under the ℓ_2 and ℓ_∞ norm. Fig. 15 and Fig. 16 show the *attack success rate vs. perturbation budget* curves of the 15 models against dodging and impersonation attacks under the ℓ_2 norm. Fig. 17 and Fig. 18 show the *attack success rate vs. perturbation budget* curves of the 15 models against dodging and impersonation attacks under the ℓ_∞ norm.

Transfer-based black-box attacks: We show the attack success rate of the 15 models against dodging and impersonation attacks based on black-box FGSM, BIM, MIM, and LGC methods under the ℓ_∞ norm in Fig. 19 and Fig. 20.

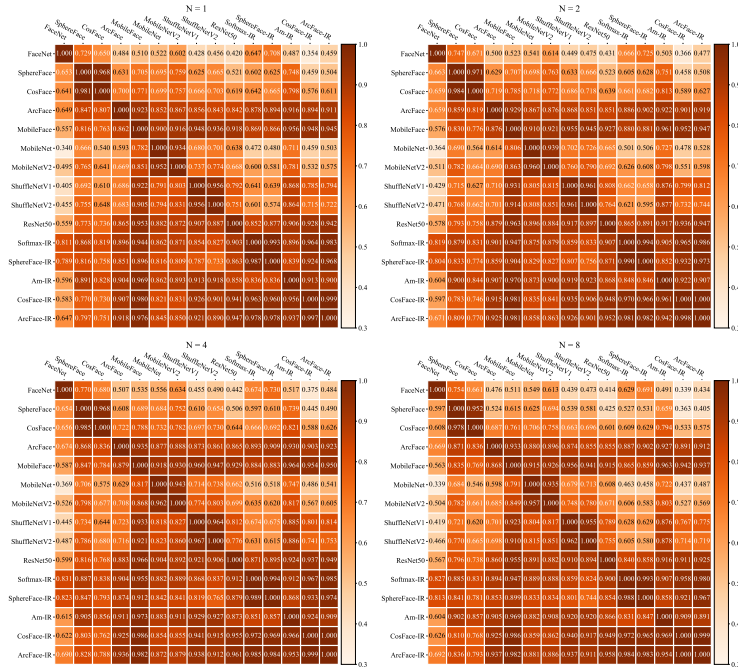


Fig. 11. The success rates of the 15 models against black-box dodging attacks under different quantities of black-squares for LGC under the l_∞ norm on LFW.

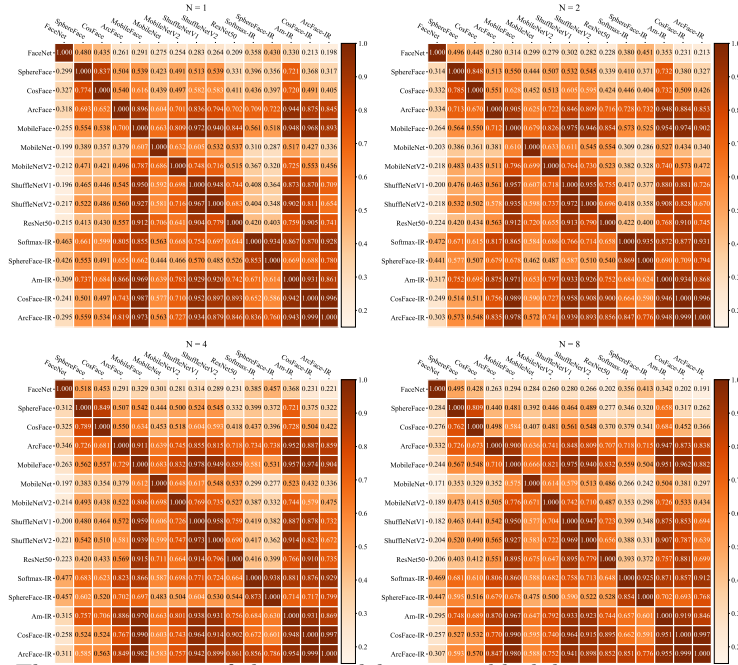


Fig. 12. The success rates of the 15 models against black-box impersonation attacks under different quantities of black-squares for LGC under the l_∞ norm on LFW.

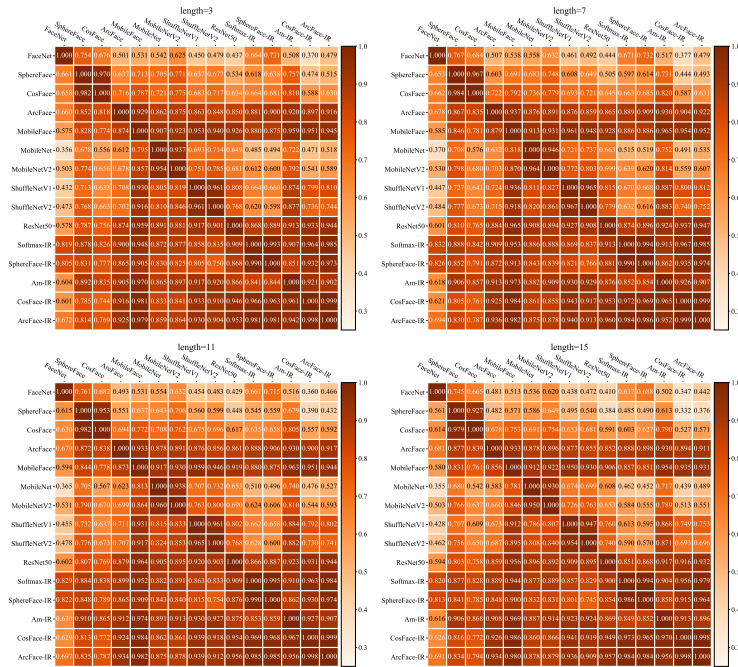


Fig. 13. The success rates of the 15 models against black-box dodging attacks under different sizes of black-squares for LGC under the ℓ_∞ norm on LFW.

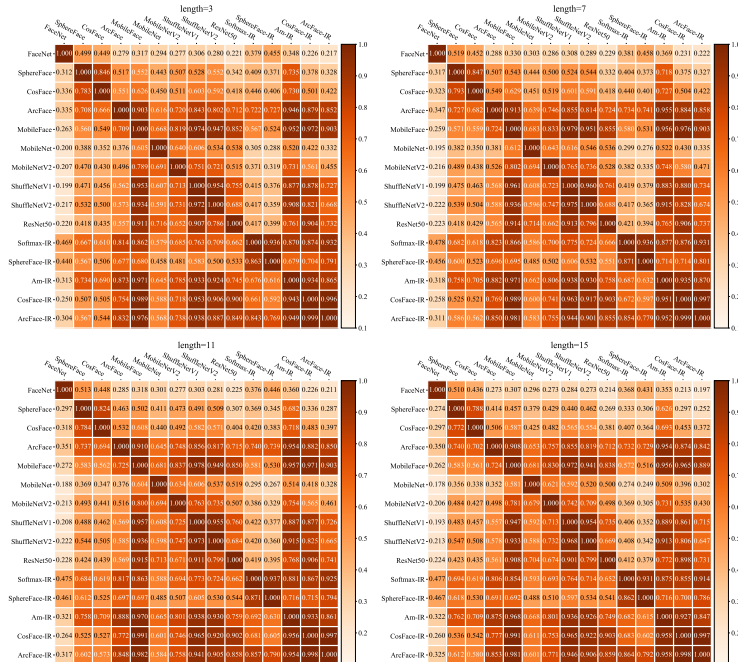


Fig. 14. The success rates of the 15 models against black-box impersonation attacks under different sizes of black-squares for LGC under the ℓ_∞ norm on LFW.

C.2 Evaluation on the CFP-FP dataset

CFP-FP dataset isolates pose variation with extreme poses like profile, where many features are occluded. The dataset contains 10 frontal and 4 profile images of 500 individuals. Similar to LFW, the standard data protocol has defined 10 splits, and contains 350 pairs with the same identities and 350 pairs with different identities.

White-box attacks: For CFP-FP dataset, we also show some robustness curves for white-box attacks and provide attack success rate vs. perturbation budget of face recognition models against dodging and impersonation attacks under the ℓ_2 and ℓ_∞ norm. Fig. 21 and Fig. 22 show the *attack success rate vs. perturbation budget* curves of the 15 models against dodging and impersonation attacks under the ℓ_2 norm. Fig. 23 and Fig. 24 show the *attack success rate vs. perturbation budget* curves of the 15 models against dodging and impersonation attacks under the ℓ_∞ norm.

Transfer-based black-box attacks: We show the attack success rate of the 15 models against dodging and impersonation attacks based on black-box FGSM, BIM, MIM, and LGC methods under the ℓ_∞ norm in Fig. 25 and Fig. 26.

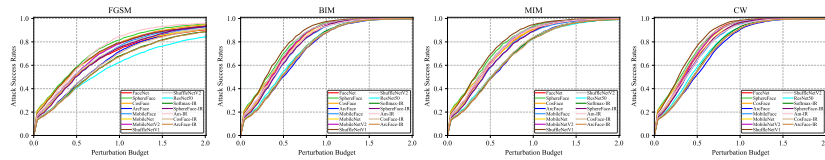


Fig. 15. The *attack success rate vs. perturbation budget* curves of the 15 models against dodging attacks under the ℓ_2 norm on YTF.

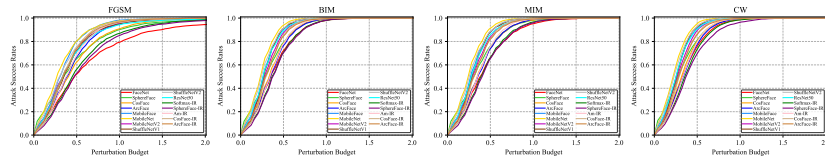


Fig. 16. The *attack success rate vs. perturbation budget* curves of the 15 models against impersonation attacks under the ℓ_2 norm on YTF.

References

1. Brendel, W., Rauber, J., Kurakin, A., Papernot, N., Velicki, B., Mohanty, S.P., Laurent, F., Salathé, M., Bethge, M., Yu, Y., et al.: Adversarial vision challenge. In: The NeurIPS’18 Competition, pp. 129–153. Springer (2020)
2. Carlini, N., Athalye, A., Papernot, N., Brendel, W., Rauber, J., Tsipras, D., Goodfellow, I., Madry, A.: On evaluating adversarial robustness. arXiv preprint arXiv:1902.06705 (2019)

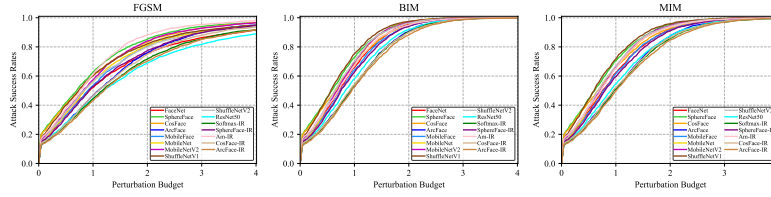


Fig. 17. The attack success rate vs. perturbation budget curves of the 15 models against dodging attacks under the ℓ_∞ norm on YTF.

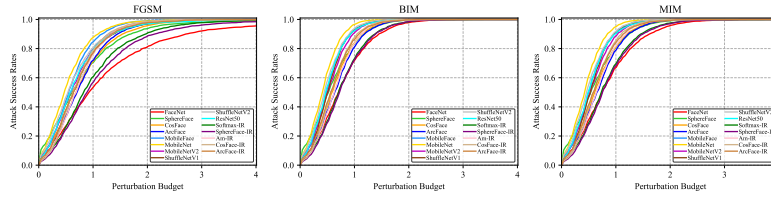


Fig. 18. The attack success rate vs. perturbation budget curves of the 15 models against impersonation attacks under the ℓ_∞ norm on YTF.

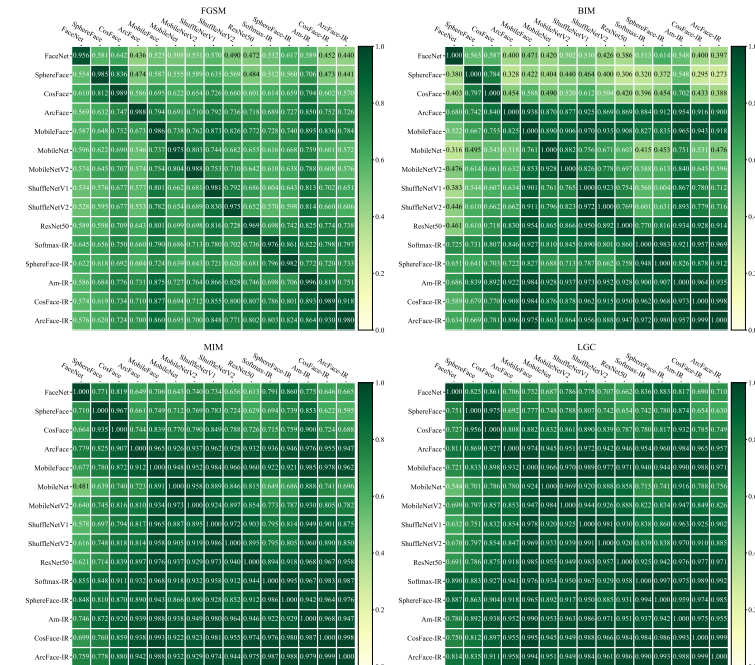


Fig. 19. The success rates of the 15 models against black-box dodging attacks under the ℓ_∞ norm on YTF.

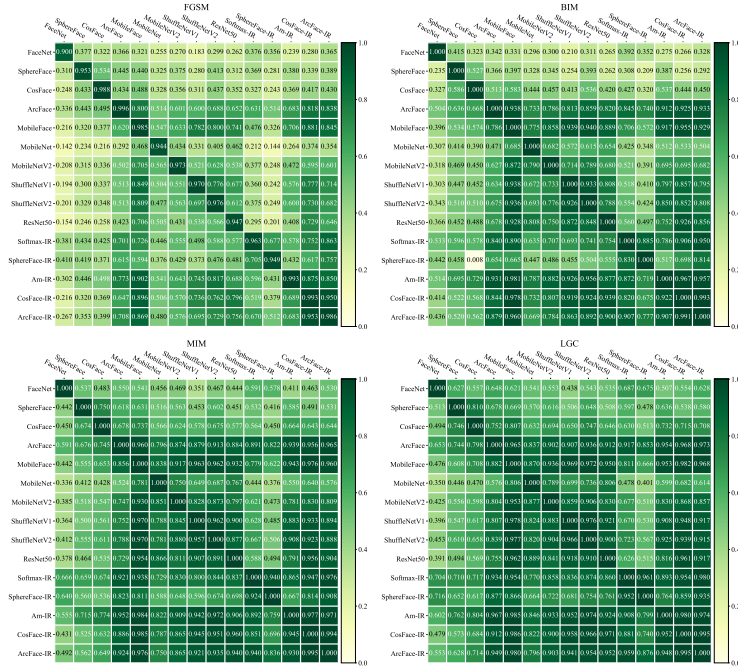


Fig. 20. The success rates of the 15 models against black-box impersonation attacks under the ℓ_∞ norm on YTF.

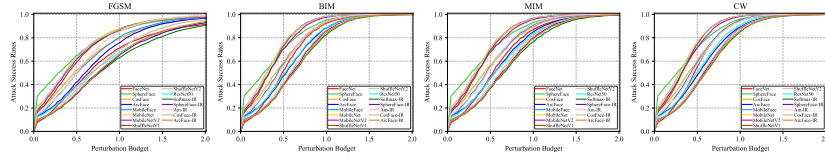


Fig. 21. The attack success rate vs. perturbation budget curves of the 15 models against dodging attacks under the ℓ_2 norm on CFP-FP.

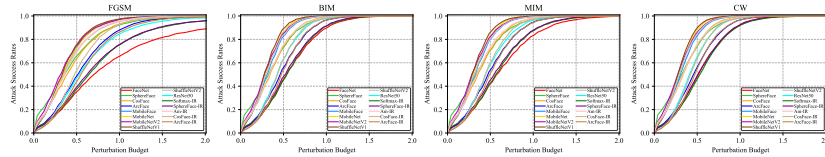


Fig. 22. The attack success rate vs. perturbation budget curves of the 15 models against impersonation attacks under the ℓ_2 norm on CFP-FP.

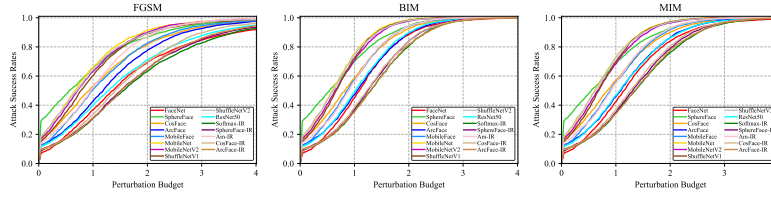


Fig. 23. The attack success rate vs. perturbation budget curves of the 15 models against dodging attacks under the ℓ_∞ norm on CFP-FP.

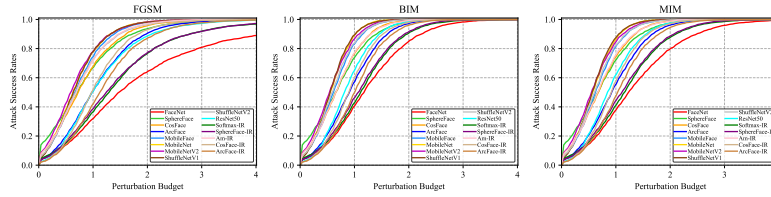


Fig. 24. The attack success rate vs. perturbation budget curves of the 15 models against impersonation attacks under the ℓ_∞ norm on CFP-FP.

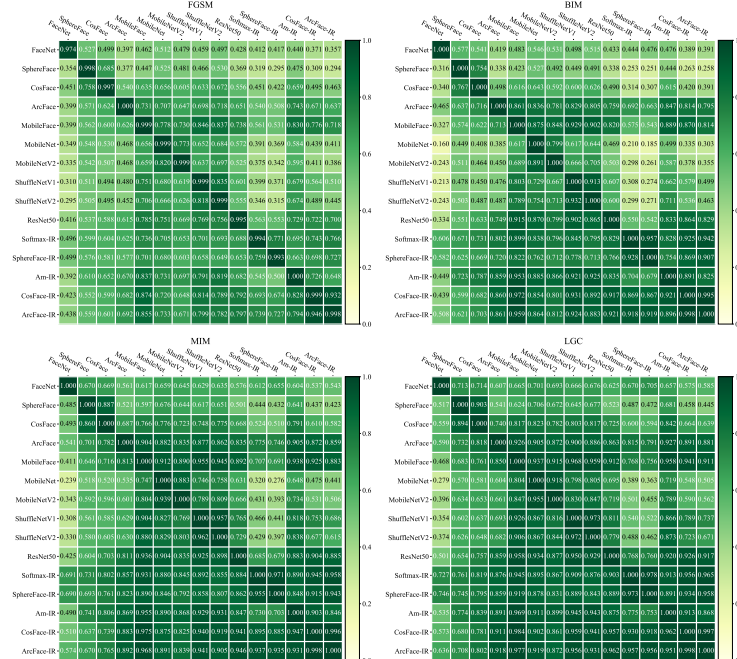


Fig. 25. The success rates of the 15 models against black-box dodging attacks under the ℓ_∞ norm on CFP-FP.

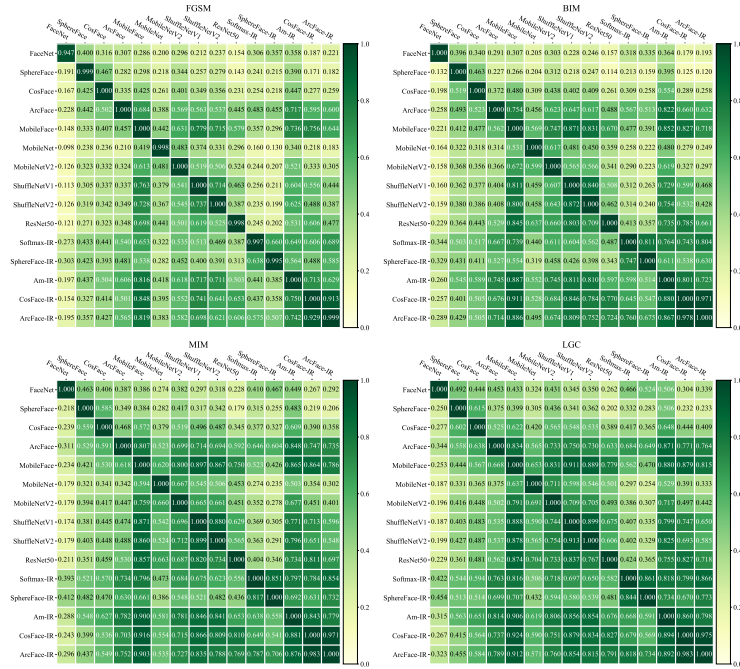


Fig. 26. The success rates of the 15 models against black-box impersonation attacks under the ℓ_∞ norm on CFP-FP.

3. Carlini, N., Wagner, D.: Towards evaluating the robustness of neural networks. In: IEEE Symposium on Security and Privacy (2017)
4. Chen, P.Y., Zhang, H., Sharma, Y., Yi, J., Hsieh, C.J.: Zoo: Zeroth order optimization based black-box attacks to deep neural networks without training substitute models. In: Proceedings of the 10th ACM Workshop on Artificial Intelligence and Security. pp. 15–26. ACM (2017)
5. Chen, S., Liu, Y., Gao, X., Han, Z.: Mobilefacenets: Efficient cnns for accurate real-time face verification on mobile devices. In: Chinese Conference on Biometric Recognition. pp. 428–438. Springer (2018)
6. Datta, R., Jia, L., Wang, J.Z.: Content-based image retrieval: approaches and trends of the new age (2005)
7. Deng, J., Guo, J., Xue, N., Zafeiriou, S.: Arcface: Additive angular margin loss for deep face recognition. In: The IEEE Conference on Computer Vision and Pattern Recognition (CVPR) (2019)
8. Deng, J., Guo, J., Xue, N., Zafeiriou, S.: Arcface: Additive angular margin loss for deep face recognition. In: Proceedings of the IEEE Conference on Computer Vision and Pattern Recognition. pp. 4690–4699 (2019)
9. DeVries, T., Taylor, G.W.: Improved regularization of convolutional neural networks with cutout. arXiv preprint arXiv:1708.04552 (2017)
10. Dong, Y., Fu, Q.A., Yang, X., Pang, T., Su, H., Xiao, Z., Zhu, J.: Benchmarking adversarial robustness. arXiv preprint arXiv:1912.11852 (2019)
11. Dong, Y., Liao, F., Pang, T., Su, H., Zhu, J., Hu, X., Li, J.: Boosting adversarial attacks with momentum. In: Proceedings of the IEEE Conference on Computer Vision and Pattern Recognition (CVPR) (2018)

12. Dong, Y., Pang, T., Su, H., Zhu, J.: Evading defenses to transferable adversarial examples by translation-invariant attacks. In: Proceedings of the IEEE Conference on Computer Vision and Pattern Recognition (CVPR) (2019)
13. Dong, Y., Su, H., Wu, B., Li, Z., Liu, W., Zhang, T., Zhu, J.: Efficient decision-based black-box adversarial attacks on face recognition. In: Proceedings of the IEEE Conference on Computer Vision and Pattern Recognition (CVPR) (2019)
14. Goodfellow, I.J., Shlens, J., Szegedy, C.: Explaining and harnessing adversarial examples. In: International Conference on Learning Representations (ICLR) (2015)
15. Guo, Y., Zhang, L., Hu, Y., He, X., Gao, J.: Ms-celeb-1m: A dataset and benchmark for large-scale face recognition. arXiv: Computer Vision and Pattern Recognition (2016)
16. Gutta, S., Philomin, V., Trajkovic, M.: An investigation into the use of partial-faces for face recognition. In: fgr. pp. 33–38 (2002)
17. He, K., Zhang, X., Ren, S., Sun, J.: Deep residual learning for image recognition. In: CVPR (2016)
18. He, K., Zhang, X., Ren, S., Sun, J.: Identity mappings in deep residual networks. In: European Conference on Computer Vision (ECCV). pp. 630–645. Springer (2016)
19. Howard, A.G., Zhu, M., Chen, B., Kalenichenko, D., Wang, W., Weyand, T., Andreetto, M., Adam, H.: Mobilenets: Efficient convolutional neural networks for mobile vision applications. arXiv preprint arXiv:1704.04861 (2017)
20. Huang, G.B., Mattar, M., Berg, T., Learned-Miller, E.: Labeled faces in the wild: A database for studying face recognition in unconstrained environments (2008)
21. Kingma, D., Ba, J.: Adam: A method for stochastic optimization. In: International Conference on Learning Representations (ICLR) (2015)
22. Kurakin, A., Goodfellow, I., Bengio, S.: Adversarial examples in the physical world. In: International Conference on Learning Representations (ICLR) Workshops (2017)
23. Kurakin, A., Goodfellow, I., Bengio, S.: Adversarial machine learning at scale. In: International Conference on Learning Representations (ICLR) (2017)
24. Liu, W., Wen, Y., Yu, Z., Li, M., Raj, B., Song, L.: Sphereface: Deep hypersphere embedding for face recognition. In: CVPR (2017)
25. Ma, N., Zhang, X., Zheng, H.T., Sun, J.: Shufflenet v2: Practical guidelines for efficient cnn architecture design. In: Proceedings of the European Conference on Computer Vision (ECCV). pp. 116–131 (2018)
26. Madry, A., Makelov, A., Schmidt, L., Tsipras, D., Vladu, A.: Towards deep learning models resistant to adversarial attacks. In: International Conference on Learning Representations (ICLR) (2018)
27. Papernot, N., McDaniel, P., Goodfellow, I., Jha, S., Celik, Z.B., Swami, A.: Practical black-box attacks against deep learning systems using adversarial examples. arXiv preprint arXiv:1602.02697 (2016)
28. Sandler, M., Howard, A., Zhu, M., Zhmoginov, A., Chen, L.C.: Mobilenetv2: Inverted residuals and linear bottlenecks. In: Proceedings of the IEEE Conference on Computer Vision and Pattern Recognition. pp. 4510–4520 (2018)
29. Schroff, F., Kalenichenko, D., Philbin, J.: Facenet: A unified embedding for face recognition and clustering. In: CVPR (2015)
30. Selvaraju, R.R., Cogswell, M., Das, A., Vedantam, R., Parikh, D., Batra, D.: Grad-cam: Visual explanations from deep networks via gradient-based localization. In: Proceedings of the IEEE international conference on computer vision. pp. 618–626 (2017)

31. Sengupta, S., Chen, J.C., Castillo, C., Patel, V.M., Chellappa, R., Jacobs, D.W.: Frontal to profile face verification in the wild. In: 2016 IEEE Winter Conference on Applications of Computer Vision (WACV) (2016)
32. Sharif, M., Bhagavatula, S., Bauer, L., Reiter, M.K.: Accessorize to a crime: Real and stealthy attacks on state-of-the-art face recognition. In: Proceedings of the 2016 ACM SIGSAC Conference on Computer and Communications Security. pp. 1528–1540. ACM (2016)
33. Sharif, M., Bhagavatula, S., Bauer, L., Reiter, M.K.: Adversarial generative nets: Neural network attacks on state-of-the-art face recognition. arXiv preprint arXiv:1801.00349 (2017)
34. Simonyan, K., Zisserman, A.: Very deep convolutional networks for large-scale image recognition. In: ICLR (2015)
35. Su, D., Zhang, H., Chen, H., Yi, J., Chen, P.Y., Gao, Y.: Is robustness the cost of accuracy?—a comprehensive study on the robustness of 18 deep image classification models. In: Proceedings of the European Conference on Computer Vision (ECCV). pp. 631–648 (2018)
36. Sun, Y., Wang, X., Tang, X.: Deep learning face representation from predicting 10,000 classes. In: CVPR (2014)
37. Szegedy, C., Liu, W., Jia, Y., Sermanet, P., Reed, S., Anguelov, D., Erhan, D., Vanhoucke, V., Rabinovich, A.: Going deeper with convolutions. In: CVPR (2015)
38. Szegedy, C., Zaremba, W., Sutskever, I., Bruna, J., Erhan, D., Goodfellow, I., Fergus, R.: Intriguing properties of neural networks. In: International Conference on Learning Representations (ICLR) (2014)
39. Taigman, Y., Yang, M., Ranzato, M., Wolf, L.: Deepface: Closing the gap to human-level performance in face verification. In: CVPR (2014)
40. Teo, C.C., Neo, H.F., Teoh, A.B.J.: A study on partial face recognition of eye region. In: 2007 International Conference on Machine Vision. pp. 46–49. IEEE (2007)
41. Tsipras, D., Santurkar, S., Engstrom, L., Turner, A., Madry, A.: Robustness may be at odds with accuracy
42. Wang, F., Cheng, J., Liu, W., Liu, H.: Additive margin softmax for face verification. *IEEE Signal Processing Letters* **25**(7), 926–930 (2018)
43. Wang, H., Wang, Y., Zhou, Z., Ji, X., Li, Z., Gong, D., Zhou, J., Liu, W.: Cosface: Large margin cosine loss for deep face recognition. In: CVPR (2018)
44. Wei, L., Rui, Z., Tong, X., Wang, X.: Deepreid: Deep filter pairing neural network for person re-identification. In: 2014 IEEE Conference on Computer Vision and Pattern Recognition (CVPR) (2014)
45. Wen, Y., Zhang, K., Li, Z., Qiao, Y.: A discriminative feature learning approach for deep face recognition. In: ECCV (2016)
46. Wolf, L., Hassner, T., Maoz, I.: Face recognition in unconstrained videos with matched background similarity. In: The IEEE Conference on Computer Vision and Pattern Recognition (CVPR) (2011)
47. Yang, X., Luo, W., Bao, L., Gao, Y., Gong, D., Zheng, S., Li, Z., Liu, W.: Face anti-spoofing: Model matters, so does data. In: Proceedings of the IEEE Conference on Computer Vision and Pattern Recognition. pp. 3507–3516 (2019)
48. Zhang, K., Zhang, Z., Li, Z., Qiao, Y.: Joint face detection and alignment using multitask cascaded convolutional networks. *IEEE Signal Processing Letters* **23**(10), 1499–1503 (2016)
49. Zhang, X., Zhou, X., Lin, M., Sun, J.: Shufflenet: An extremely efficient convolutional neural network for mobile devices. In: Proceedings of the IEEE Conference on Computer Vision and Pattern Recognition. pp. 6848–6856 (2018)